Indian Journal of Engineering & Materials Sciences
Vol. 30, February 2023, pp. 122-131
DOI: 10.56042/ijems.v1i1.46198

Instability Regions of a laminated Sandwich Plate with MRE Core Under Parametric Excitation Using Finite Element Method

Hafiz Mayeen[a], Rajesh Kumar Ojha[b*], & Santhosha Kumar Dwivedy[c]

[a]Indian Oil Corporation Limited, R & D centre, Sector-13, Faridabad, Haryana 121 007, India
[b]University College of Engineering and Technology, Bikaner, Rajasthan 334004, India
[c]Indian Institute of Technology Guwahati, Assam 781 039, India

Received: 9 February 2021; Accepted: 21 March 2022

This paper is concerned with the instability regions of a laminated sandwich plate with magneto-rheological elastomer (MRE) core under periodic axial loads. Structures operating under this unstable region cause large response even if the excitation force is small in magnitude. The governing equations of motion of the system are obtained by using finite element method [FEM].The parametric stable and unstable regions of the MRE cored composite sandwich plate for different system parameters and end constraints are found using modified Hsu method for simple parametric resonance condition. This analysis will help to design passive attenuation by using sandwich plates of varied dimensions, material parameters of both skin and core. Further active vibration reduction is possible by applying suitable magnetic field and operating the system outside of the instability region.

Keywords: Finite element method, Modified Hsu method, MRE core, Sandwich plate, Simple resonance

1 Introduction

Composite sandwich structures find applications in many industries due to light weight with improved mechanical properties than the monolithic structures. Basic unit of composite sandwich structure consists of soft elastomeric core with thin stiff composite material layered on both sides. Multilayered sandwich plates are used depending upon application. For active vibration control system, the sandwich plate with MRE core can be used. This MRE core consists of rheological particles whose orientation can be varied under different external magnetic field.

Zhou and Wang[1] have studied the effects of conductive skin in the MRE sandwich plates. Ray and Nayak et al[2] have studied the free vibration analysis and parametric instability regions of sandwich beams. Kar[3] have studied the parametric instability of multilayered sandwich beam. Yousuf and Rasid[4] have analysed the parametric stability of viscoelastic cored sandwich plate using FEM. Ray and Kar et al[5] have determined the parametric instability region of a sandwich beam with viscoelastic core using higher order theory. Lin and Chen[6] have studied the dynamic stability of rotating composite beam and pre twisted blades with constrained damping layers. Ojha and Dwivedy[7,8] have analysed the dynamic behaviour of viscoelastic cored sandwich plate with isotropic/ composite skins using FEM. Dwivedy et al.[9] have carried out the parametric stability analysis of the sandwich beam with softcore analytically. Kao et al.[10] have investigated the parametric instability behaviour of foam filled sandwich structure using Bolotin method. Yeh[11] has discussed the parametric vibration of axisymmetric annular sandwich plate using the Bolotin method. Sofiyev et al.[12] have investigated parametric instability of the cylindrical shaped sandwich shell using Bolotin method. Ramamoorthy et al.[13] have studied the vibration of the sandwich plate with magneto rheological core. Ojha and Dwivedy[15] have discussed instability regions of sandwich plate with LPRE viscoelastic core under parametric loading for different end constraints, using FEM and modified Hsu method. Quac et al[16] have studied the dynamic response of sandwich plate with honey comb structured core layer having negative Poisson's ratio. Gao et al [17] have analysed the dynamic behaviour of sandwich structure plate with functionally graded porous material skins and core layer made of viscoelastic material. Rafi et al[18] have discussed the dynamic analysis of the hybrid sandwich

*Corresponding author (E-mail-rajeshkumarojha07@gmail.com)

plate with skin layers made of composite material integrated with piezoelectric material. D at et al[19] have investigated the dynamic behaviour of a sandwich plate with functionally graded CNT reinforced skin.

Upon rigorous literature review, it is recognized that no work has been outlined on parametric instability study on sandwich plate with MRE[5] core.MRE is used in sandwich panel to actively suppress the vibration in structures. Here, the parametric instability regions of the sandwich plate with MRE[5] core is discussed in detail.

2 Materials and Methods

The finite element method for parametric instability analysis of the sandwich plate is discussed in the section. The three-layered MRE cored sandwich plate with composite skins is shown in Fig. 1. No slip between the interface surfaces occurs. Top and bottom layers are stiff and core layer is a soft material. The skin layers of sandwich plate undergo tension/ compression due to transverse load and core layer carries shear load. The skin layers are mathematically modelled using classical plate theory. Failure due to delamination is neglected since the epoxy used in binding the interface layer is stronger than the foam.

2.1 Mathematical Formulation

The axial force, $P(t) = P_0 + P_1 \cos \omega t$ is applied on the sandwich plate as shown in Fig. 2. The deformed shape of the sandwich plate due to axial loading is shown in Fig. 3.

The displacement field of in plane and out plane for the top skin layer is written.

$$u_t(x,y,z,t) = u_{0t}(x,y,t) - z\frac{\partial w}{dx}$$

$$v_t(x,y,z,t) = v_{0t}(x,y,t) - z\frac{\partial w}{dy} \quad \ldots (1)$$

where,

u_t displacement field in x direction of top skin,
v_t displacement field in y direction of top skin,
w transverse displacement field

The displacement field of in plane and out plane for the bottom skin layer is written.

$$u_b(x,y,z,t) = u_{0b}(x,y,t) - z\frac{\partial w}{dx}$$

$$v_b(x,y,z,t) = v_{0b}(x,y,t) - z\frac{\partial w}{dy} \quad \ldots (2)$$

where,

u_b displacement field in x direction of bottom skin,
v_b displacement field in y direction of bottom skin

The transverse displacement is considered same throughout the depth of the plate.

$$w = w(x,y,t) \quad \ldots (3)$$

The core layer in plane and out plane displacement field is written.

$$u_c(x,y,z,t) = (u_c{}^{bot} - u_c{}^{top})\frac{z}{c} + u^{top}{}_c$$

$$v_c(x,y,z,t) = (v_c{}^{bot} - v_c{}^{top})\frac{z}{c} + v_c{}^{top}$$

$$w_c = w(x,y,t) \quad \ldots (4)$$

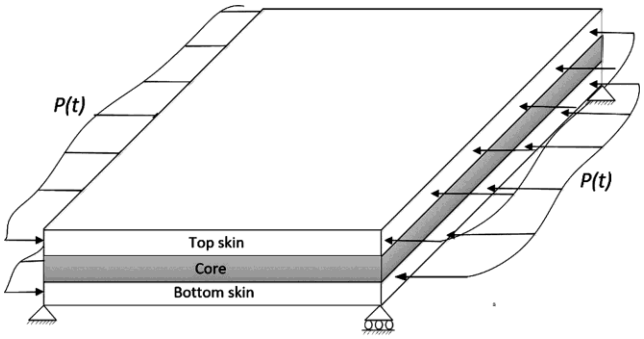

Fig. 2 — Sandwich plate under periodic axial loading in x-direction

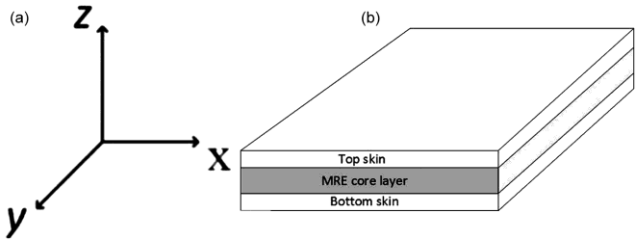

Fig. 1 — Sandwich plate with MRE core layer.

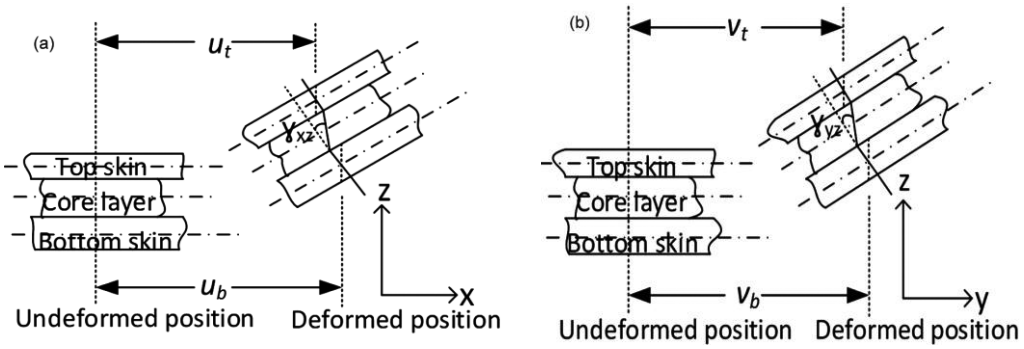

Fig. 3 — Deformed and undeformed position of the sandwich plate (a) x-z plane (b) y-z.

The expression of kinetic energy (T_{KE}) of the plate is written[7,8]

$$T_{KE} = \frac{1}{2}\iint_{\Omega} \rho_t h_t \left(\left(\frac{\partial u_t}{\partial t}\right)^2 + \left(\frac{\partial v_t}{\partial t}\right)^2 + \left(\frac{\partial w}{\partial t}\right)^2 \right) dxdy + \frac{1}{2}\iint_{\Omega} \rho_b h_b \left(\left(\frac{\partial u_b}{\partial t}\right)^2 + \left(\frac{\partial v_b}{\partial t}\right)^2 + \left(\frac{\partial w}{\partial t}\right)^2 \right) dxdy + \frac{1}{2}\iint_{\Omega} \rho_c h_c \left(\left(\frac{\partial u_{0c}}{\partial t}\right)^2 + \left(\frac{\partial v_{0c}}{\partial t}\right)^2 + \left(\frac{\partial w}{\partial t}\right)^2 \right) dxdy \quad \ldots (5)$$

2.2 Expression of the potential Energy

The stress and strain relationship of the laminate with different angle is given.

$$\begin{bmatrix} \sigma_x \\ \sigma_y \\ \tau_{xy} \end{bmatrix} = \begin{bmatrix} \overline{Q}_{11} & \overline{Q}_{12} & \overline{Q}_{16} \\ \overline{Q}_{12} & \overline{Q}_{22} & \overline{Q}_{26} \\ \overline{Q}_{16} & \overline{Q}_{26} & \overline{Q}_{66} \end{bmatrix} \begin{bmatrix} \varepsilon_x \\ \varepsilon_y \\ \gamma_{xy} \end{bmatrix} \quad \ldots (6)$$

where, $\begin{bmatrix} \varepsilon_x \\ \varepsilon_y \\ \gamma_{xy} \end{bmatrix} = \begin{bmatrix} \varepsilon_{0x} \\ \varepsilon_{0y} \\ \gamma_{0xy} \end{bmatrix} + z \begin{bmatrix} \kappa_x \\ \kappa_y \\ \kappa_{xy} \end{bmatrix}$ … (7)

The $\left[\overline{Q}\right]$ is determined as mentioned in Ojha and Dwivedy[8] works.

$$U_{PE} = \frac{1}{2}\iint_{\Omega} \{\varepsilon_{0i}\}^T \begin{vmatrix} [A_i] & [B_i] \\ [B_i] & [D_i] \end{vmatrix} \{\varepsilon_{0i}\} dxdy + \frac{h_2}{2}\iint_{\Omega} \{\gamma_{xz} \quad \gamma_{yz}\}^T \begin{bmatrix} G & 0 \\ 0 & G \end{bmatrix} \begin{Bmatrix} \gamma_{xz} \\ \gamma_{yz} \end{Bmatrix} dxdy \quad \ldots (8)$$

where,

$$\{\varepsilon_{0i}\}^T = \left| \frac{\partial u_{0i}}{\partial x} \quad \frac{\partial v_{0i}}{\partial y} \quad \frac{\partial u_{0i}}{\partial y} + \frac{\partial v_{0i}}{\partial x} \quad -\frac{\partial^2 w}{\partial x^2} \quad -\frac{\partial^2 w}{\partial y^2} \quad -2\frac{\partial^2 w}{\partial x \partial y} \right|,$$

'*i*' stands for top and bottom skins, U_{PE} is the potential energy of the plate and G is the Shear Modulus of MRE core layer[20].

$$(A_i)_{kl} = \sum_{m=1}^{n} \left[(\overline{Q}_{kl})\right]_m (h_m - h_{m-1}),\ k = 1,2,6;\ l = 1,2,6$$

$$(B_i)_{kl} = \frac{1}{2}\sum_{m=1}^{n} \left[(\overline{Q}_{kl})\right]_m \left(h^2{}_m - h^2{}_{m-1}\right),\ k = 1,2,6;\ l = 1,2,6 \quad (5)$$

$$(D_i)_{kl} = \frac{1}{3}\sum_{m=1}^{n} \left[(\overline{Q}_{kl})\right]_m \left(h^3{}_m - h^3{}_{m-1}\right),\ k = 1,2,6;\ l = 1,2,6$$

The work done by the axial periodic force is,

$$W = \frac{1}{2}\iint_{\Omega} P(t)\left(\frac{\partial w}{\partial x}\right)^2 dxdy \quad \ldots (9)$$

The four-nodded element with twenty-eight degrees of freedom for finite element model of the sandwich plate is discussed[8].

$$u_{0t} = N_1 u_{0t1} + N_2 u_{0t32} + N_3 u_{0t3} + N_4 u_{0t4}$$
$$v_{0t} = N_1 v_{0t1} + N_2 v_{0t2} + N_3 v_{0t3} + N_4 v_{0t4}$$
$$u_{0b} = N_1 u_{0b1} + N_2 u_{0b2} + N_3 u_{0b3} + N_4 u_{0b4}$$
$$v_{0b} = N_1 v_{0b1} + N_2 v_{0b2} + N_3 v_{0b3} + N_4 v_{0b4} \quad \ldots (10)$$

The expression for transverse displacement of the plate are written.

$$w = N_5 w_1 + N_6 \frac{\partial w_1}{\partial x} + N_7 \frac{\partial w_1}{\partial y} + N_8 w_2 + N_9 \frac{\partial w_2}{\partial x} + N_{10} \frac{\partial w_3}{\partial y} + N_{11} w_3 + N_{12} \frac{\partial w_3}{\partial x} + N_{13} \frac{\partial w_3}{\partial y} + N_{14} w_4 + N_{15} \frac{\partial w_4}{\partial x} + N_{16} \frac{\partial w_4}{\partial y} \quad \ldots (11)$$

N_5, N_8, N_{11}, N_{14} are the shape functions for the transverse displacement at nodes 1, 2, 3, 4 respectively.

N_6, N_9, N_{12}, N_{15} are the shape functions for the slope about Y axis at nodes 1, 2, 3, 4 respectively.

$N_7, N_{10}, N_{13}, N_{16}$ are the shape functions for the slope about X axis at nodes 1, 2, 3, 4 respectively[15].

The relationship between displacement variable, nodal degrees and shape function is written as,

$$\{u_t \quad v_t \quad u_b \quad v_b \quad w\}^T = [N]_{5\times 28}\{q^e\}_{28\times 1} \quad \ldots (12)$$

The elemental stiffness matrix of the sandwich plate is written.

These elemental mass and stiffness matrix are assembled to get the global mass and stiffness matrix and the governing equation of motion is written as,

$$[M]\{\ddot{f}\} + [K]\{f\} - P_1 \cos\omega t[F]\{f\} = \{\phi\} \quad \ldots (13)$$

Here, $[M]$ is the mass matrix, $[K]$ is the complex matrix due to viscoelastic property of MRE[5] and as well as changes with externally applied magnetics load. $[F]$ is the force matrix.

Using the above presented mathematical formulation, a code has been developed in the MATLAB for the further analysis, which is to be carried out.

2.3 Parametric instability conditions

The parametric instability region of the system is determined by using modified Hsu's method. Simple resonance condition is considered to define the instability regions of the plate under the effect of axial periodic loading.

When the excitation frequency is equal to two times of the natural frequency, principal parametric resonance appears[21].

Simple Resonance type

$$\left|\frac{\bar{\omega}}{2} - \omega_{\lambda,R}\right| < \frac{1}{4}\chi_\lambda \quad \ldots (14)$$

where, $\chi_\lambda = +\left[\frac{4\varepsilon^2(b^2{}_{\lambda\lambda,R} + b^2{}_{\lambda\lambda,I})}{\omega^2{}_{\lambda,R}} - 16\omega^2{}_{\lambda,I}\right]$

where, $\chi_{\lambda\nu} = \frac{\omega_{\lambda,I}\omega_{\nu,I}}{4(\omega_{\lambda,I}\omega_{\nu,I})^{1/2}}\left[\frac{4\varepsilon^2(b_{\lambda\nu,R}b_{\nu\lambda,R} + b_{\lambda\nu,I}b_{\nu\lambda,I})}{\omega_{\lambda,R}\omega_{\nu,R}} - 16\omega_{\lambda,I}\omega_{\nu,I}\right]^{1/2}$

Also, $[b] = -P_1[L]^{-1}[M]^{-1}[F][L]$

where, ω^2 is the eigenvalue and L is the eigenvector of $[M]^{-1}[K]$. b and ω contains real and imaginary parts.

3 Results and Discussion

The MATLAB code has been developed based on the mathematical modelling. The parametric instability regions are found for different boundary conditions and system parameters. These parameters include thickness of core, thickness of composite skin, effect of magnetic field, ply orientation of composite skin, storage modulus, loss factor and length and width of the plate. The geometrical and material property for the study is taken from the Table 1 otherwise it is mentioned. The experimental shear modulus of MRE core is considered from Nayak et al.[2].

The graphite epoxy laminate material of skins property is considered in the instability analysis of the plate and written.

Young's Modulusin longitudinal direction, $E_x = 137$ GPa;

Young's Modulus in transverse direction, $E_y = 8.96$ GPa;

Modulus of rigidity in x-y plane, $G_{xy} = 7.1$ GPa ;

Poisson ratio, $\nu_{xy} = 0.3$; Poisson ratio, $\nu_{yx} = 0.3$;

3.1 Validation of the FEM code

The FEM code is compared with the analytical solution in the available literatures. The natural frequency obtained from FEM code is compared with the results from literatures[7,8]. The material and geometric properties taken for the comparison purpose are shown in the Table 2.

lenght (l) =0.348m, breadth (b) =0.0348, loss factor (η) =0.5 .

The boundary conditions used is simply supported boundary condition.

$$At\ x = 0\ and\ x = l, \quad u_j, v_j, w, \frac{\partial w}{dy} = 0 \qquad \text{where, } j\text{=top,bot}$$

Table 1 — Geometric and material properties for the sandwich plate

	Top skin	Bottom skin	Core
Thickness	1 mm	1 mm	1 mm
Density	1600 kg/m^3	1600 kg/m^3	3312.7 kg/m^3
Length(l) x Breadth(b)	0.4m x 0.3m	0.4m x 0.3m	0.4m x 0.3m

Table 2 — Geometrical and material properties for the sandwich plate

	Top skin	Bottom skin	Core
Thickness	0.762 mm	0.762 mm	0.254 mm
Density	2740 kg/m^3	2740 kg/m^3	999 kg/m^3
Young's Modulus	68.9 GPa	68.9 GPa	0.869 GPa

$$At\ y=0\ and\ x=b,\quad u_j, v_j, w, \frac{\partial w}{dx}=0 \qquad \text{where, } j\text{=top,bot}$$

The natural frequencies found using the developed MATLAB code is very close with results from the literature and is presented in the Table 3.

3.2 Effect of different composite skins thicknesses on instability regions of simply supported sandwich plate

The nature of the parametric instability regions for the variation of the thickness of the skin layers are studied here. Figure 4 shows the shift in instability region due to the variation in skin thickness. Fig. 5 (a) & (b) shows the unstable response of the system when the operating regions inside the instability curve (point B) and Fig. 5 (c) shows the stable response curve for the sandwich plate operating outside the instability curve (point A and C).

With the increase in skin thickness, the instability region is shifting towards higher dynamic loads. By keeping thicker skin layers, system can be safely operated under higher dynamic loads for any frequency.

The stable and unstable regions of a plate with different skin thickness for a simply supported boundary condition up to the first three modes are plotted in Fig. 6. Here, the axial periodic force is applied to the plate.

At every mode with the increase in the skin thickness, parametric instability regions are shifted towards the higher loads. Critical load at first mode was at 11.04 kN and it is increased to 11.17kN with 0.01 mm increase in top and bottom skin. Parametric instability for the first mode is found at higher loads for simply supported boundary condition. At third mode, instability regions are shifted to lower dynamic loads compared to the second mode. At second mode critical load was found at 33.17 kN and at third mode it was found at 6.05 kN for the skin thickness of 1 mm.

3.3 Effect on parametric instability due to variation in thickness of MRE core layer for simply supported sandwich plate

MRE core layer defines the damping characteristics of the sandwich plate. The shifting of parametric instability regions for different core thickness are studied here and plotted in Fig. 7.

With the increase in core thickness, the stability of the system is improved. The unstable region is shifting towards the higher dynamic loads. For 1 mm core thickness, critical load is found at 3.65 kN and it increased to 3.75 kN and 3.85 kN with an increase of 0.01 mm. The instability regions are slightly shifting towards lower frequency regions with the increase in core thickness. At second mode, critical load of

Table 3 — Comparison of the natural frequencies of the present analysis with available benchmark results.

	Natural Frequency(Hz)		
	Present analysis	Ojha[7]	Ojha[8]
Mode 1	62.1	60.3	57.4
Mode 2	113.8	115.4	113.2
Mode 3	128.2	130.6	130.6

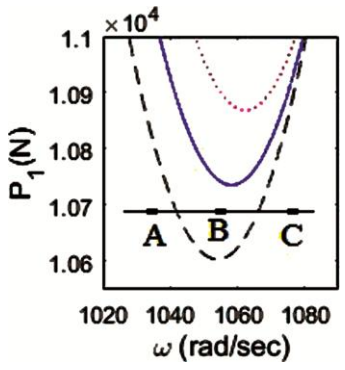

Fig. 4 — Parametric instability region for the variation in the skin thickness for mode 1for different skin thickness.

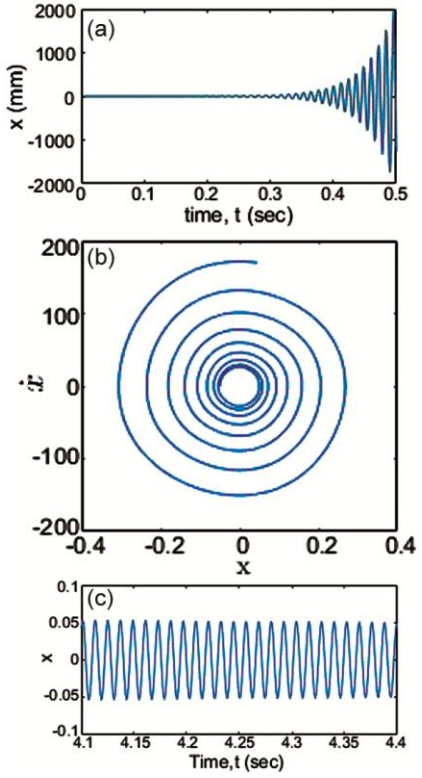

Fig. 5 — (a) Unstable response of the system at point B, (b) Phase portrait of the system at point B, and (c) Stable response of the system at point A.

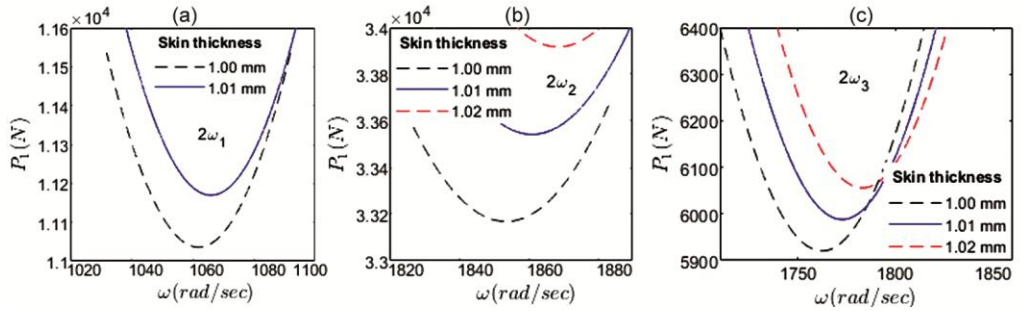

Fig. 6 — Parametric instability region up to third mode for different skin thickness for simply supported boundary condition at (a) First mode, (b) second mode, and (c) third mode.

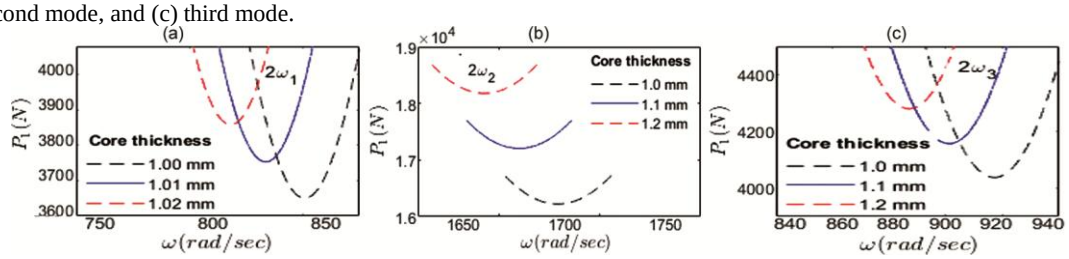

Fig.7 — Parametric instability regions up to third mode for the variation in core thickness for simply supported boundary condition at (a) First mode, (b) second mode, and (c) third mode.

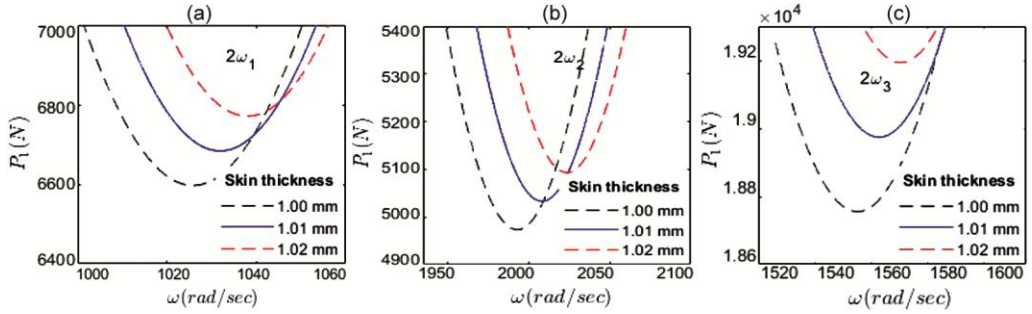

Fig. 8 — Parametric instability regions up to third mode for the variation in skin thickness for all sides clamped boundary condition at (a) First mode, (b) second mode, and (c) third mode.

16.23 kN is found and at third mode, critical load dropped to 4.03 kN.

3.4 Effect on parametric instability due to variation in thickness of composite skins for all side clamped sandwich plate

Parametric instability region for the first three modes are plotted in the Fig. 8 for a sandwich plate with 1mm core thickness and with all sides clamped boundary condition.

The parametric instability regions are shifting towards the higher dynamic loads with the increase in the skin thickness. The instability regions are observed at 6.59 *kN* and increased to 6.68 *kN* for 0.01*mm* increase of skin thickness for the first mode. Instability regions are shifted towards higher frequency also. The instability regions are shifted to lower loads at second mode. Critical load is found to be 4.97 *kN* for 1 *mm* skin thickness. Critical load is increased to 18.76 kN at third mode. This trend is contrast from the results of sandwich plate with simply supported boundary condition.

3.5 Effect on parametric instability due to thickness of composite skins for left end fixed and other ends free sandwich plate

The parametric stability regions for first, second and third modes are plotted in Fig. 9 for the plate with distinct stiff skin thickness for left side fixed and other ends free sandwich plate.

Shift of parametric regions towards higher loads are observed with the increase in skin thickness. Parametric instability regions are found at much lower dynamic loads for this boundary condition compared to the simply supported boundary condition and all sides clamped boundary condition. Critical load is found at 382.5 kN for 1 mm skin thickness. It is slightly increased to 390.9 N with the increase of 0.01 mm and to 400.3 N with further .01 mm increase. Instability regions are shifted to higher loads

for second mode and then shifted to lower loads at third mode. Critical load is found at 1.77 kN at the second mode and 1.40 kN at third mode for the 1 mm skin thickness.

3.6 Effect on parametric instability due to variation in magnetic field for all sides clamped sandwich plate

Parametric instability regions up to the first third mode for the variation in magnetic field for all sides clamped boundary condition are studied here and plotted in the Fig. 10.

For the given boundary condition, the parametric loads are shifted toward higher loads up to second mode and then dropped to lower loads at the third mode, which is similar to the results observed for the simply supported boundary condition. Critical loads are lesser compared to the critical loads with simply supported boundary conditions with other parameters same. In the absence of the magnetic field, the critical load is found at 10.1 kN at the first mode, 5.85 kN at the second mode and increased to 32.82 kN at the third mode.

3.7 Effect on parametric instability due to variation in magnetic field for one side fixed and other ends free sandwich plate

Parametric instability regions up to the third mode for the variation in magnetic field for one side clamped and other ends free sandwich plate are plotted in the Fig. 11.

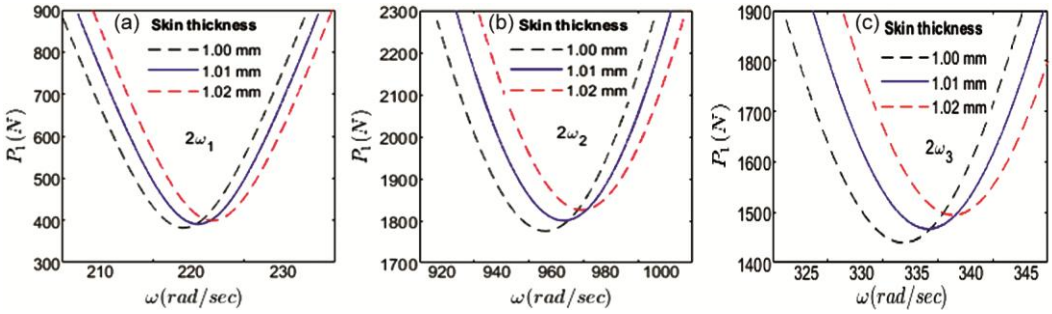

Fig. 9 — Parametric instability regions up to third mode for the variation in skin thickness for left end fixed and other ends free boundary condition at (a) First mode, (b) second mode, and (c) third mode.

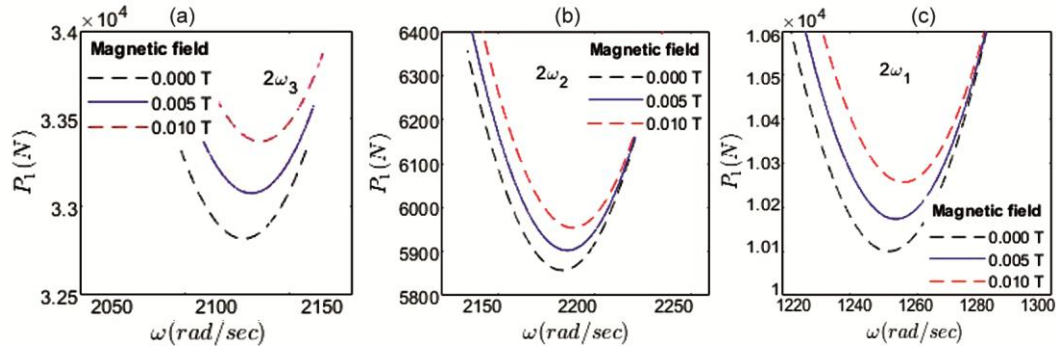

Fig. 10 — Parametric instability region for the first three modes for the variation in magnetic field for all sides clamped boundary condition at (a) First mode, (b) second mode, and (c) third mode.

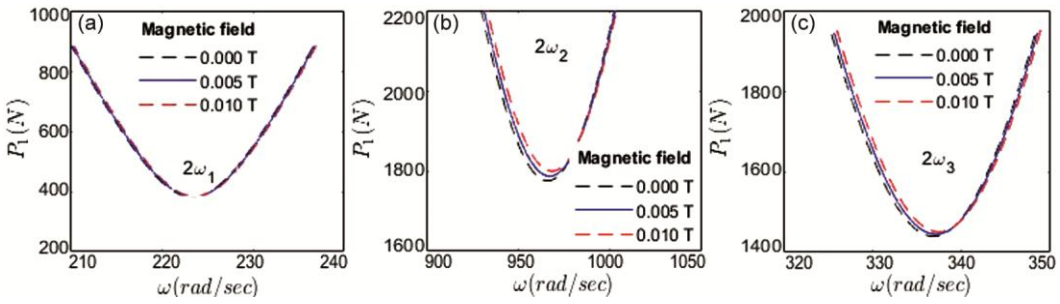

Fig. 11 — Parametric stability regions for first, second and third modes of a plate with variation in magnetic field for one side fixed and other ends free boundary condition at (a) First mode, (b) second mode, and (c) third mode.

Comparing to the other boundary conditions, the variation in the magnetic field is not affected much in the instability regions. At second mode, instability regions are found at higher dynamic loads compared to the first and third mode. In the absence of magnetic field, at first mode critical load is found at 382.2 N. With increase of 0.005 T magnetic field, the critical load is slightly increased to 382.9 N. In the second mode, critical load is found at 1.78 kN and decreased to 1.45 kN in the absence of magnetic field.

3.9 Effect on parametric instability due to variation in length for simply supported sandwich plate

The length of the sandwich plate is one of the constraints that limit the design. The shifting of parametric instability region for different length are studied for a square plate. Parametric instability regions for the sandwich plate with simply supported boundary condition for the variation in the length are plotted in Fig. 12.

With the increase in length of the plate, the parametric regions are shifted towards lower loads. Parametric instability regions are dropped at second mode and shifted to higher loads at third mode. For the $0.3\,m \times 0.3\,m$ cross section, the critical load is found at 7.39 kN in the first mode. As the length of all sides are increased by 5 mm the critical load is dropped to 7.34 kN. For the $0.3\,m \times 0.3\,m$ cross section, critical load of 5 kN is found at second mode and 19.31 kN at the third mode.

3.10 Effect on parametric instability due to variation in length for all edges fixed sandwich plate

The parametric instability regions for the sandwich plate up to third mode with all edges fixed constraints for the variation in the length are plotted in Fig. 13.

The parametric instability regions are found to shift towards lower dynamic loads with the increase in the length of the plate. For the $300\ mm \times 300\ mm$ cross section, the critical load is found at $6.7kN$ in the first mode. As the length of all sides are increased by $5\ mm$ the critical load is dropped to $6.65kN$. Instability regions shift towards lower loads at second mode and increases to higher loads at third mode. Instability regions are shifted towards lower frequencies with the increase in length of the plate. At second mode, parametric instability regions are found at lower loads compared to first and third mode. For the $300\ mm \times 300\ mm$ m cross section, critical load of $5.01kN$ is found at second mode and $18.92kN$ at the third mode.

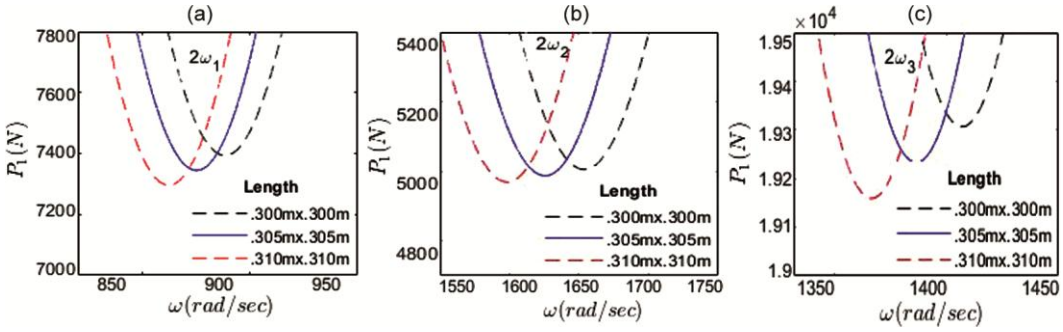

Fig. 12 — Parametric stability regions up to first three modes with variation in length of sandwich plate for simply supported boundary condition at (a) First mode, (b) second mode, and (c) third mode.

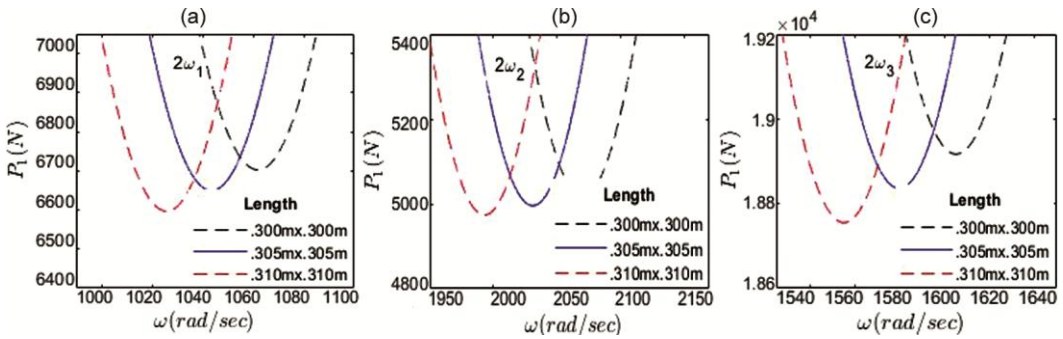

Fig. 13 — Parametric instability regions for the first three modes for the variation in length of the plate for all edges fixed boundary constraints at (a) First mode, (b) second mode, and (c) third mode.

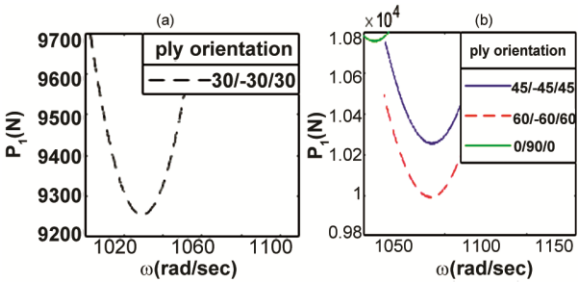

Fig. 14 — Parametric instability regions for different ply orientations for a simply supported boundary condition (a) 30/-30/30 ply orientation, (b) 45/-45/45, 60/-60/60, and 0/90/0 ply orientation.

3.11 Effect on parametric instability due to different ply orientation for simply supported sandwich plate

The properties of composite skin also depend upon the ply orientation. The shifting of parametric instability region for different ply orientation (0/90/0, 30/-30/30, 45/-45/45, 60/-60/60) are studied and plotted in Fig. 14.

Figure 14 is plotted for the first mode. For ply orientation 30/-30/30, instability regions are found at lower dynamic loads. The critical loads are found at 9.25 kN for this ply orientation. 0/90/0 is found to be more stable at higher loads. Critical load for 0/90/0 are found at 10.75 kN. Parametric instability regions for the 45/-45/45 and 60/-60/60 are found near to the instability regions of 0/90/0 and critical loads are found at 10.25 kN and 9.99 kN respectively.

4 Conclusion

The governing equation of motions has been developed for the three layered sandwich plate with MRE core layer and composite skin layers. The developed FEM MATLAB code has been validated with the available literature and found to be with good agreement. Hence, the parametric instability analysis of the sandwich plate is carried out by using this MATLAB code. Parametric instability regions have been plotted using modified Hsu method for different parameters such as core thickness, skin thickness, length and width of plate, magnetic field intensity under three different boundary conditions. Parametric stability study for simple resonance conditions up to third mode are also studied.

The fundamental natural frequency of the sandwich plate in the absence of magnetic field is found to be 98.77 Hz for all sides clamped boundary condition. With the application of 0.2 T magnetic field on the sandwich plate, fundamental frequency is increased by 13.8 % and loss factor increases by 24.98%. For magnetic field of 0.4 T and 0.6 T, an increase of 25.12% and 28.89 % was observed in natural frequency. When both the skin thickness is reduced by 0.5 mm, natural frequency decreases by 28.95% and loss factor increases by 9.69 %. When both the skin thickness is increased by 0.5 mm, natural frequency increases by 30.8 % and loss factor decreases by 16.97 %. When the core thickness is reduced by 0.5 mm, natural frequency increases by 14.85 % and loss factor decreases by 13.88 %. When the core thickness is increased by 0.5 mm, natural frequency decreases by 7.69 % and loss factor increases by 8 %. For 0.3m x 0.3 m cross-section the natural frequency and loss factor are found to be 127.60 Hz and 0.1145. When the cross section is increased to 0.6 m x 0.6m, natural frequency decreases by 63.59 % and loss factor increases by 2 %. The response of the system is found to be decreasing with the increase in the magnetic fields. The loss modulus of the MRE core layer is increased with the increase in magnetic field.

In the study of the parametric vibration of the sandwich plates following observations are made. One side clamped and other ends free boundary condition has lower critical load compared to the other boundary conditions, which can be avoided under parametric excitation. All side simply supported or all sides clamped boundary condition shows instability regions at higher dynamic loads compared to other boundary conditions. Stability of the system can be improved with the increase in loss factor as the instability region is shifted to higher dynamic loads. Principal parametric regions are observed to be shifting towards the higher dynamic loads as the thickness of the skins and the core is increased. Increase in length of the sandwich plate makes the system unstable at lower dynamic loads.0/90/0 ply orientation is preferred over the other orientation since unstable regions are shifted towards higher dynamic loads. Hence the study can be extended to industrial designs of any structures with flexible core with stiff skins operating under dynamic loading applications to avoid unstable responses. The weight of the MRE cored sandwich plate is found 2.35 times lesser than the iron cored sandwich plate and fulfil the purpose of controlling the eternal excitations using different magnetic fields. The loss factors of MRE embedded sandwich plate is found more than the sandwich plates with core made of conventional material and is due to the complex shear modulus of the MRE core.

References

1 Zhou G Y & Wang Q, *Smart Mater Struct*, 14 (2005) 1001
2 Nayak B, Dwivedy S K & Murthy K S R K, *J Sound Vib*, 330 (2011) 1837
3 Ray K & Kar R C, *J Sound Vib*, 193 (3) (1996) 631
4 Yus of Z & Rasid Z A, *AIP Conference Proceedings*, 1750 (2016) 030044
5 Ray K & Kar R C, *Comput Struct*, 60 (1996) 817
6 Lin CY & Chen LW, *Compos Struct*, 61(2003) 235
7 Ojha RK & Dwivedy SK, *Int J Struct Stab Dyn*, 19 (2019) 1950033
8 Ojha RK & Dwivedy SK, *J Vib Eng Technol*, 8 (2020) 541
9 Dwivedy S K, Sahu K C & Babu S K, *J Sound Vib*, 304 (2007) 326
10 Kao J Y, Chen C S & Chen W R, *Mech Compos Mater*, 48 (2012) 765
11 Yeh J Y, *Smart Struct Syst*, 8 (2011) 487
12 Sofiyev A H & Kuruoglu N, *Int J Mech Sci*, 20 (2015), 7403
13 Ramamoorthy M, Rajamohan R & Jeevanantham A K, *J Vib Control*, 22(2014) 869.
14 Dwivedy S K & Sahu K C,*J Sound Vib*, 304 (2007) 326
15 Ojha R K & Dwivedy SK, *J Sandw Struct Mate*, *23*(8) (2021) 3685
16 Quoc T H, Tu T M & Van Tham V, *J Sc Tech in Civil Eng*, 15(4) (2021) 1
17 Gao Z, Li H, Zhao J, Guan J & Wang Q, *Eng Struc*, 248 (2021) 113242
18 Rafi S S, Alam M N & Rahman N, *Mater Today Proc*,46(19) (2021) 10009
19 Dat N D, Thanh N V, Minh Anh V & Duc N D, *Mech Adv Mater & Struct*, (2020) 1
20 Kaw A K, Mechanics of Composite material (CRC Taylor and Fransis, London), 2nd Edn, ISBN: 0849313430, 9780849313431, p. 100
21 Saito H & Otomi K, *J Sound Vib*, 63 (1979) 169